Available online at www.sciencedirect.com

ScienceDirect

Energy Procedia 55 (2014) 94 – 100

Energy Procedia

4th International Conference on Silicon Photovoltaics, SiliconPV 2014

Optimized back reflectors for rear diffused c-Si solar cells

Andrea Ingenito[a,*], Juan Camilo Ortiz Lizcano[a], Stefan L. Luxembourg[b], Rudi Santbergen[a], Arthur Weeber[b], Olindo Isabella[a] and Miro Zeman[a]

[a]*Photovoltaic Materials and Devices Laboratory / Dimes, Delft University of Technology, The Netherlands*
[b]*ECN Solar Energy, Petten, The Netherlands*

Abstract

At present, research in c-Si solar cells is focused on increasing the efficiency while reducing the amount of used materials. Since silicon wafer and metal contribute up to 50% to the cost of a module, it is crucial to reduce the amount of these materials to fabricate cost-effective modules. In particular, for reducing the consumption of metal, the rear back contact can be patterned leaving ample metal-free regions that are well passivated. This is the concept of open-rear-metallization, typically found in solar cell concepts such as n-Pasha. In this contribution we compare a Distributed Bragg Reflector (DBR), white paint and white foil as cost-effective back reflectors for rear diffused c-Si solar cells.

© 2014 Published by Elsevier Ltd. This is an open access article under the CC BY-NC-ND license (http://creativecommons.org/licenses/by-nc-nd/3.0/).
Peer-review under responsibility of the scientific committee of the SiliconPV 2014 conference

Keywords: back reflector; distributed Bragg reflector; white paint; absorption

1. Introduction

It has been shown that silicon wafer and metal contribute up to 50% of the total fabrication costs of a PV module [0]. An obvious way to decrease the costs related to employed materials is minimizing their use. However, less silicon absorber material results in a reduced absorption of light in silicon. In addition to such incomplete photon absorption, the major optical losses in c-Si solar cells are the front reflection and parasitic absorption in the back metal reflector. In order to enhance the conversion efficiency, light trapping schemes are applied to minimize these optical losses. A typical light trapping scheme in industrial state-of-the-art c-Si solar cells consists of: (i) randomly roughened front and rear surfaces for

* Corresponding author. Tel.: +31-15-2788905; fax: +31-15-2782968.
E-mail address: a.ingenito@tudelft.nl

1876-6102 © 2014 Published by Elsevier Ltd. This is an open access article under the CC BY-NC-ND license (http://creativecommons.org/licenses/by-nc-nd/3.0/).
Peer-review under responsibility of the scientific committee of the SiliconPV 2014 conference
doi:10.1016/j.egypro.2014.08.085

light scattering, (ii) anti-reflection coating (ARC) [0] for enhancing the light in-coupling at the front side and (iii) aluminium as back reflector (BR). Internal back reflectance of the standard evaporated Al back reflectors on Si is around 80%, while back reflectance larger than 90% can be achieved by using the more expensive Ag together with a thick oxide layer between the Si and the BR [0]. This means that in such optimal case, at least 10% of the light reaching the back side of the solar cell is absorbed in the BR. Alternatively, metal-free BRs could be used in solar cell concepts like n-Pasha [0], where the rear metallic back contact can be patterned leaving ample regions coated by the passivation layer. In this work we present the design and fabrication of three efficient, metal-free and cost-effective BRs applied in an open rear-metallization configuration. In particular, we propose the usage of an omni-directional dielectric Distributed Bragg Reflector (DBR) [0,0], TiO_2 particles used as white paint (WP) [0] and white foil (WF) Trosifol R40 Ultra White [0] in the role of perfect mirror for rear diffused c-Si solar cells. Moreover, in this work we focused on the comparison of measured optical performances reflectance (R), transmittance (T) and absorptance (A) for the three presented BRs.

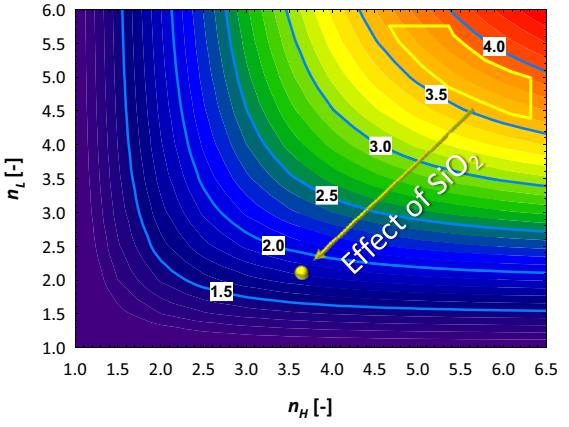

Fig. 1. First omni-directionality condition: $n_0' > n_0$ [0]. Light blue lines on the contour plot are iso-value curves indicating the refractive index of the incident medium (n_0) on top of the DBR. Inserting a SiO_2 layer ($n_0 = n_{SiO2(1000\ nm)} = 1.5$) between the bulk c-Si and the DBR allows for the use of existing non-absorbing materials at $\lambda_B = 1000$ nm like a-SiN_x:H ($n_{L(1000\ nm)} = 1.76$, $d_{a\text{-}SiNx:H} = 146$ nm) and a-Si:H ($n_{H\ (1000\ nm)} = 3.61$, $d_{a\text{-}SiN:H} = 69$ nm).

2. Design of omni-direction DBR

A DBR is formed by pairs of alternating dielectric layers with refractive index mismatch. Such multi-layer stack delivers high reflectance in a certain wavelength range around the so-called Bragg wavelength (λ_B). The most stringent requirement for a DBR to be used as BR is to achieve the highest internal back reflectance ($R_b = 1$) in the wavelength range of weak absorption of c-Si and independently from the angle of incidence and the polarization of light. These two conditions have to be fulfilled to achieve the so-called omni-directional behaviour [0]. The first condition of omni-directionality is met if:

$$n_0' = \frac{n_H\, n_L}{\sqrt{n_H^2 + n_L^2}} > n_0 \qquad (1)$$

where n_0 is the refractive index of the incident medium and n_H (n_L) is the high (low) refractive index of each material constituting the DBR couple. To verify equation 1 for a DBR - $n_0' = f(n_L, n_H)$ - having bulk c-Si as incident medium (n_0) (see yellow area in Fig. 1), non-absorbing materials with high n_L and n_H refractive indexes at $\lambda_B = 1000$ nm are required. Instead, inserting a SiO_2 layer ($n_0 = n_{SiO2(1000\ nm)} = 1.5$) between the bulk c-Si and the DBR allows for the use of existing non-absorbing materials at $\lambda_B = 1000$ nm like a-SiN_x:H ($n_{L(1000\ nm)} = 1.76$) and a-Si:H ($n_{H\ (1000\ nm)} = 3.61$). Using optical modelling based on 3-D finite element method [0], we simulated the optical system

presented in figure 2a and we determined the minimum number of a-Si:H / a-SiN_x:H pairs and the individual layer thicknesses that resulted in $R_b = 1$ and verified the omni-directional behaviour of our dielectric DBR. As reported in Fig. 2b this was achieved by using six pairs of a-Si:H / a-SiN_x:H with respective thicknesses of 69 nm and 145 nm.

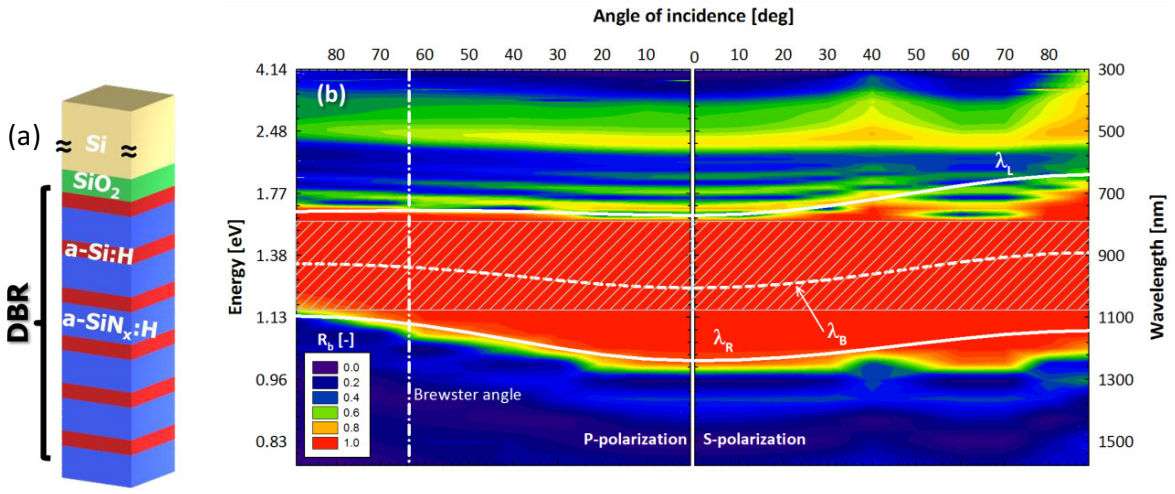

Fig. 2. (a) Simulated structure and (b) calculated internal reflectance for different angles of incidence and for P-polarization and S-polarization. The shaded area represents the omni-directional photonic band-gap (second omni-directionality condition). The white horizontal solid and dashed curves are the angle dependent photonic band edges (λ_L and λ_R) and the Bragg wavelength, respectively. In the P-polarization panel, the vertical dash-dotted line locates the Brewster angle of the optical system.

3. Fabrication of back reflectors

Float Zone (FZ) p-type wafers with resistivity 1-to-5 Ω-cm and thickness around 285 µm were used as absorber material. The wafers were textured on both sides in an alkaline bath based on TMAH and IPA. After texturing, a 75-nm thick SiN layer was deposited on both sides of the wafers via Plasma Enhanced Chemical Vapour Deposition (PE-CVD). In addition, for all fabricated samples an additional 75-nm thick layer of SiO_2 deposited via PE-CVD was deposited at the back side (see Fig. 3a). As shown in the previous section, this layer is necessary in case of DBR BR to fulfill the first condition of omni-directionality. However, in order to have a fair comparison between all BRs we deposited this layer for all configurations of BRs.

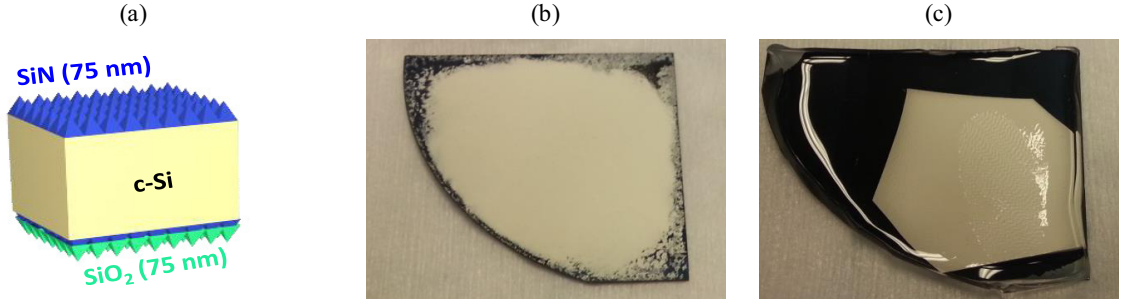

Fig. 3. (a) Schematic structure of the fabricated samples prior the deposition of the BR (b) White paint drop casted or (c) PDMS + WF applied at the back side of textured sample with SiN / SiO_2 stack as illustrated in (a).

An Elettrorava cluster tool was used to deposit the 6 pairs of a-Si:H / a-SiN_x:H constituting the DBR with modeled thicknesses of 69 and 145 nm, respectively. In Fig. 4, scanning electron microscopy (SEM) images of the deposited DBRs are presented. The SEM images also report the directions orthogonal to the pyramid facet (X-direction) and parallel to PE-CVD direction growth (Y-direction). Fig. 4a shows the cross-sectional SEM of the designed DBR (called DBR 1) deposited on a polished surface. The image clearly shows the 6 pairs of a-Si:H / a-SiN_x:H with thicknesses of 68 and 162 nm respectively. The same DBR was co-deposited on alkaline textured surface (see Fig. 4b). As such figure clearly shows, the thicknesses of the individual layers in Y-direction are very close to the one deposited on flat surface, while in X-direction they are scaled of a geometrical factor with respect to Y-direction. The factor is equal to 1.7 and can be calculated as $1/\sin(90-\theta)$, where $\theta = 54.7°$ in case of alkaline random texturing (see definition of θ in Fig. 4c). Therefore, in order to achieve the desired thicknesses of a-Si:H / a-SiN_x:H in X-direction for alkaline textured surfaces, we increased the deposition time by the same geometrical factor. This led to the so-called DBR 2, whose layer thicknesses in Y-(X-)direction of a-Si:H and a-SiN_x:H measured around 300 nm (181 nm) and 120 nm (73 nm) (see Fig. 4c and Fig. 4d). These thicknesses are compatible with modeled ones within the acceptable deposition dis-uniformity [**0**]. For the application of WP at back side of the sample sketched in Fig. 3a, we drop casted TiO_2 particles mixed in H_2O with ratio 1:10 followed by drying in air for 12 hours [**0**] (see Fig. 3b). In particular, a thickness larger than 50 µm was found to be sufficient to ensure a T < 5 % at 1200 nm [**0**]. Finally, polydimethylsiloxane (PDMS) was used to encapsulate the WF (see Fig. 3c) at the back side of the textured sample sketched in Fig. 3a.

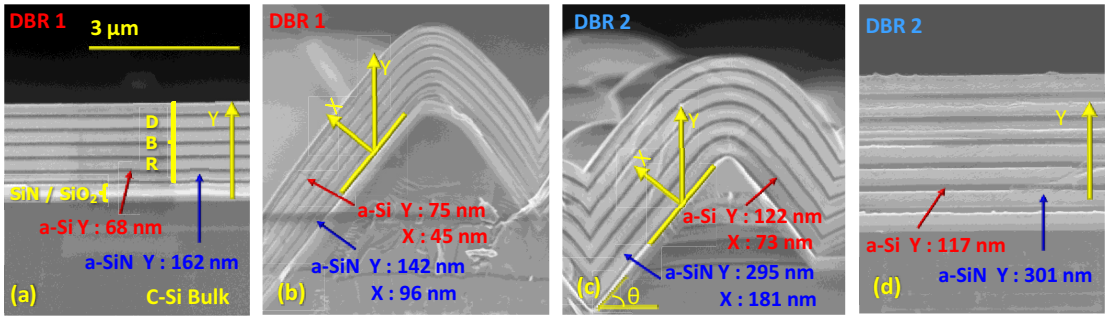

Fig. 4. Cross sectional SEM of DBR 1 deposited on flat and textured surfaces (a) and (b). X and Y axis indicates the directions orthogonal to the pyramid facet and parallel to the PECVD deposition growth, respectively. In order to achieve the desired layer thicknesses of 69 nm (a-Si:H) and 145 nm (a-SiNx:H) on textured surfaces (c) deposition time was increased of a factor equal to 1.7. The DBR 2 deposited on flat surfaces is shown in (d).

4. Results and discussion

An integrating sphere (IS) mounted on a Perkin-Elmer spectrophotometer was used to measure R and T in the wavelength between 350 and 1200 nm. Total absorption was calculated as 1-R-T. This quantity equals the absorptance in Si (A_{Si}) (including parasitic absorption of SiN between 350 and 400 nm) for all BRs except in case of WF BR, which shows parasitic absorption in the NIR (A_{WF}). Therefore, in case of the WF BR sample, an analytical model was deployed to calculate A_{Si} from the measured R [0]. In order to confirm the validation of the optical simulations, we applied the SiO_2 / DBR 1 (see Fig. 4 (a)) of section 2 as BR of a double side polished (DSP) wafer. As Fig. 5 depicts, the simulated DBR when applied on a DSP wafer is able to deliver a R of 100% and a T equal to 0% for wavelength longer than 1000 nm (weak absorption range for silicon) as expected from optical simulations. Fig. 6 and Fig. 7 (a) and (b) depict the measured spectra (R, A_{Si}, T and A_{WF}) presented in this work. As expected, the BR only influences the near infrared (NIR) spectra of A_{Si}. The WF leads to the poorest A_{Si} response in the NIR due to its high parasitic absorption as illustrated in the inset of Fig. 7 (a) and (b). A comparable A_{Si} spectrum was achieved by using the DBR 1, optimized for flat surfaces, as BR as reported in Fig. 5. On the contrary to the WF

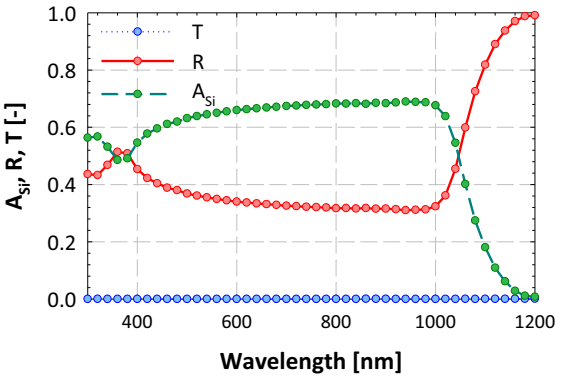

Fig. 5. A_{Si}, R,T measured for a DSP sample with SiO_2 (100 nm) / DBR 1 stack (see Fig. 4 (a)) in the wavelength range between 350 and 1200 nm.

which showed T = 0 in the region of weak Si absorption, the major optical loss of the DBR 1 is related to transmittance. As already discussed in the previous section, this DBR is not optimized for textured surfaces. Transmittance losses of the DBR were reduced by 50% increasing the deposition time of a factor 1.7 (DBR 2) see section 3. This led to a clear enhancement of the A_{Si} in the NIR response when compared to DBR1 and WF. Finally, the WP BR shows T around 3% at 1200 nm (see Fig. 7 (a) and (b)), leading to the highest A_{Si} in the NIR region (see Fig. 6). One can notice that even though the T decreases from 14% to 3% at 1150 nm when switching from DBR 2 to WP, the A_{Si} at 1150 nm decreases only from 43% to 39 %.

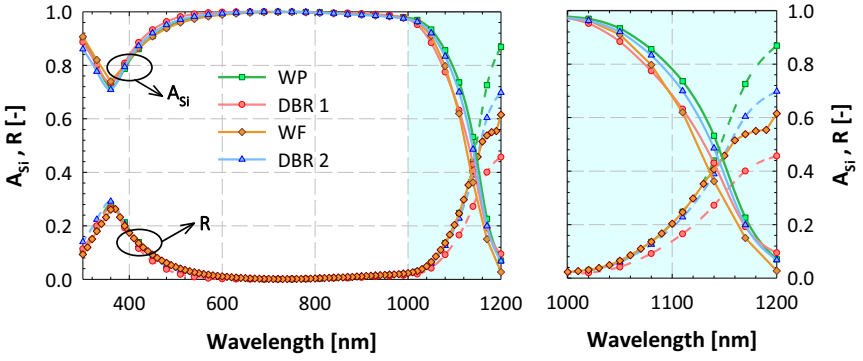

Fig. 6. (a) A_{Si} and R measured for all BRs investigated in the wavelength range between 350 and 1200 nm. (b) Detail of A_{Si} and R measured for all BRs investigated in the wavelength range between 1000 and 1200 nm. Both DBR 1 and WF show poor A_{Si} in the NIR region due to high T and high A_{WF}, respectively. Improved A_{Si} in the NIR was achieved instead by using WP or DBR 2.

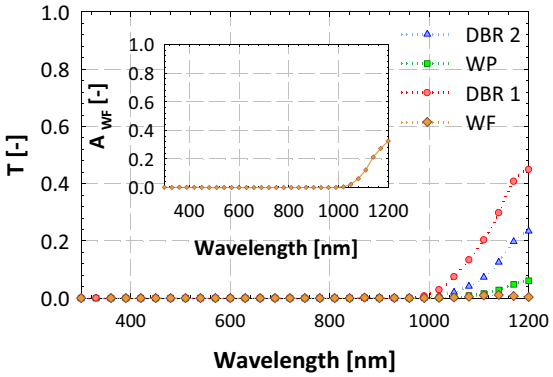

Fig. 7. T measured for all BRs investigated in the wavelength range between 350 and 1200 nm. The inset shows the calculated absorption in the WF (A_{WF}) applied at back side of the sample in Fig. 3c as function of the wavelength.

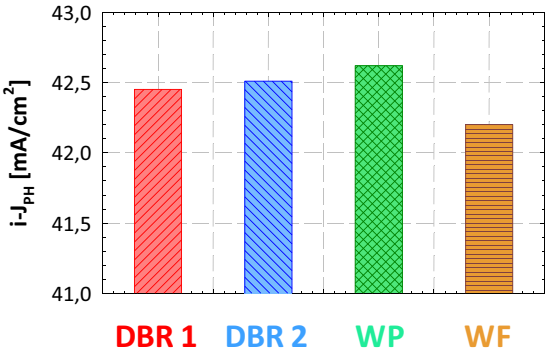

Fig. 8. Implied photo-generated current density (i-J_{PH}) calculated by integrating the product of the AM 1.5 spectrum and the measured absorptances in the wavelength range between 350 and 1200 nm. i-J_{PH} higher than 42.5 mA/cm^2 where achieved in case of DBR2 and WP BRs.

To conclude, in Fig. 8 we report the implied photo-generated current density (i-J_{PH}) calculated by integrating the product of the photon flux of the AM 1.5 ($\Phi_{AM\,1.5}$) spectrum and A_{Si} of each BR in the wavelength range between 350 and 1200 nm according to the following equation:

$$\text{i-}J_{PH} = -q \cdot \int_{350}^{1200} A_{Si}(\lambda) \cdot \Phi_{AM1.5}(\lambda) d\lambda \qquad (2)$$

Finally, i-J_{PH} higher than 42.5 mA/cm^2 was achieved in case of DBR 2. In particular, a difference of only +0.1 mA/cm^2 i-J_{PH} was observed between WP and DBR 2. Such small difference derives from the low value of the absorption coefficient of Si in the region of weak absorption.

5. Conclusions

In this work we designed and implemented four BRs suitable for open rear diffused c-Si solar cells. For DBR deposited via PE-CVD technique deposition time needs to be increase of a factor 1.7 in order to achieve the desired thicknesses in the direction orthogonal to the pyramids facets. By increasing the deposition time used for DBR 1 and DBR 2 the measured rear-side transmittance decreased by 50%. However, transmittance losses still amounted to approximately 23% at a wavelength of 1200 nm. Therefore, further investigations using ray tracing optical simulator are required to optimize the design of DBR for textured surfaces. Ultra-white foil from Trosifol showed considerable absorption in the NIR region, which makes it not an optimal choice as BR for open rear diffused c-Si solar cells. WP drop casted showed the lowest optical losses leading to the highest silicon absorption in the NIR region. Despite the better optical performance of the WP with respect to the DBR, to our knowledge, tools for mass production are not readily available. On the other hand, tools for the deposition of a-Si:H and a-SiN_x:H for large scale application are already used by silicon photovoltaic industry.

Acknowledgements

Authors acknowledge Hairen Tan for helping with SEM images, Fai Tong Si and Martijn van Sebille for helping with DBR deposition. This work was carried out within the AdLight project founded by Agentschap NL.

References

[1] Goodrich A, Woodhouse M, Hsu D. Si Solar Manufacturing Cost Models. http://www.nrel.gov/docs/fy12osti/53938.pdf ; 2011.
[2] Zhao J, Wang A, Altermatt P, Green M A. 24% efficient silicon solar cells with double layer antireflection coatings and reduced resistance loss. Appl. Phys. Lett 1995; 66:3636-3638.
[3] Campbell P, Green M A. Light trapping properties of pyramidally textured surfaces. J. Appl. Phys 1987; 62: 243-249.
[4] Romijn I G, Gutjahr A, Saynova D S, Anker J, Kossen E J, Tool K. Cost effective n-Pasha solar cells with efficiency above 20%. Photovoltaics International 2013; 20: 33-40.
[5] Isabella O. Light management in thin-film silicon solar cells. Delft University of Technology, PhD thesis, ISBN: 978-94-6203-279-8; 2013.
[6] Ingenito A, Isabella O, Zeman M. Experimental Demonstration of 4n2 Classical Absorption Limit in Nanotextured Ultrathin Solar Cells with Dielectric Omnidirectional Back Reflector. ACS Photonics 2014; 1:270-278.
[7] Santbergen R, Blanker J, Dhathathreyan A, Tan H, Smets A H M, Zeman M. Towards Lambertian internal light scattering in solar cells using coupled plasmonic and dielectric nanoparticles as back reflector. Photovoltaic Specialists Conference (PVSC) 2013; 29-33
[8] http://www.trosifol.com/en
[9] http://rredc.nrel.gov/solar/spectra/am1.5/